Radiocarbon, Vol 61, Nr 1, 2019, p 51–65 DOI:10.1017/RDC.2018.75

HOLOCENE PRECIPITATION RECORDS FROM INNER MONGOLIA DERIVED FROM HYDROGEN ISOTOPE COMPOSITIONS OF SEDIMENT FATTY ACIDS

Qingmin Chen[1] • Weijian Zhou[2*] • Zhe Wang[1] • Feng Xian[2] • George S Burr[2]

[1]Shaanxi Center of Geological Survey, Shaanxi Institute of Geological Survey, Xi'an 710068, China.
[2]State Key Laboratory of Loess and Quaternary Geology, Institute of Earth Environment, Chinese Academy of Sciences, Xi'an 710061, China.

ABSTRACT. The Inner Mongolian Plateau lies along the northern limit reached by the East Asian summer monsoon. This geographic setting makes it especially sensitive to environmental change and an excellent site for understanding Quaternary East Asian monsoon variability. In this study we present new results of hydrogen isotopic compositions of fatty acids extracted from sediments, which were used to construct Holocene paleoprecipitation (or moisture) changes in Northern China. The hydrogen isotopic composition (D/H ratio) of *n*-acids in the sedimentary sequence of the Duoerji peat, Inner Mongolia, was determined with gas chromatography and mass spectrometry. Changes in the precipitation from middle Inner Mongolia are recorded by the D/H ratio of *n*-C_{20}, *n*-C_{22}, *n*-C_{24}, *n*-C_{26}, *n*-C_{28} acids (δD). From 10–9 ka, the relatively high δD values indicate reduced precipitation in the Early Holocene. Subsequently, increased precipitation is reflected by reduced δD values from 9–5.5 ka. After 5.5 ka, gradually increasing δD values record an overall decrease in precipitation. The precipitation trends established for the Duoerji sequence are consistent with other major paleoclimate proxies in the East Asian monsoon region, especially with a distinct Holocene optimum of increased monsoonal activity from 9–5.5 ka. The δD resulting paleo-precipitation record clearly shows that the Holocene climate in Northern China is basically controlled by the insolation changes.

KEYWORDS: Duoerji, East Asian monsoon, hydrogen isotopes, *n*-fatty acids, precipitation records.

INTRODUCTION

The Holocene is the most important geological era for cultures and human society (An et al. 2000; Ruddiman 2008), which makes it extremely important to understand the mechanisms driving Holocene climate change. However, controversies still exist regarding the mechanism for Holocene climate change. In the Asian monsoon region, many speleothem and paleolimnology records suggest that the variation of monsoon intensity generally followed the summer insolation (Zhou et al. 2004; Wang et al. 2005). However, the implication of the oxygen isotope ($\delta^{18}O$) in speleothems has been questioned (Clemens et al. 2010; Liu et al. 2014). In addition, the timing of the Holocene optimum in North China remains unclear (Shi et al. 1992; An et al. 2000; Liu et al. 2002; Chen et al. 2003, 2008; Wang et al. 2005; Guan et al. 2010; Jiang et al. 2014). The Inner Mongolia Plateau is located along the northern margin of East Asian monsoon influence, which is especially sensitive to changes in the monsoon influence. Thus establishing high-quality records of climate change in the Inner Mongolia during the Holocene, especially precipitation records, is extremely helpful to understand the mechanism for climate change in the East Asian monsoon region, to some extent, which is also helpful to support the significance of speleothem $\delta^{18}O$ records to the precipitation change of Asian monsoon from another perspective.

Scientists have made substantial progress in understanding the Holocene climate variability in North China using a variety of sediment climate proxies such as pollen, grain size, magnetic parameters, and geochemical characteristics (Liu et al. 2002; Xiao et al. 2004; Peng et al. 2005; Sun et al. 2009; Wen et al. 2010; Guan et al. 2010; Yin et al. 2011; Zhai et al. 2011; Wang et al. 2012; Xu et al. 2013; Jiang et al. 2014). However, there is a need to improve our understanding by studying additional environmental proxies that are sensitive to a broader range of paleoenvironmental parameters. Pioneering studies have demonstrated that the original information is preserved by lipid molecular fossils during long periods of burial (Bray et al. 1961; Eglinton et al. 1967; Logan et al. 1995). These molecular fossils contain a plentiful record

*Corresponding author. Email: weijian@loess.llqg.ac.cn.

of diverse paleoenvironmental information. They do not suffer from some of the limitations imposed on other proxies, such as the long distance transport of exogenous pollen, or poor preservation of large fossils, which can obscure paleoenvironmental sediment records (Cranwell 1973; Brassell et al. 1986; Ishiwatari et al. 1994; Ficken et al. 1998; Mügler et al. 2008; Seki et al. 2009; Zhou et al. 2010; Nelson et al. 2013). D/H ratios of leaf waxes (δD_{wax}) derived from terrestrial plants and preserved in lake sediments can provide important information on past continental hydrology. Ideally, δD_{wax} is a well-established paleoclimate proxy that can be used to reconstruct precipitation D/H ratios (δD_P) (Hou et al. 2008; Seki et al. 2009).

In this study we present the hydrogen isotopic compositions (D/H ratio) of *n*-acids from a sedimentary sequence in central Inner Mongolia. These data are coupled with accelerator mass spectrometry (AMS) ^{14}C dates to establish a firm chronological framework and reconstruct the evolution of paleovegetation and precipitation in middle Inner Mongolia. Regional climate change characteristics are also discussed for the Holocene, in the context of global climate change occurring at that time.

SAMPLES AND METHODS

Study Site

The Duoerji peat bog (40°39.867′N, 111°1.480′E, 1022 m above sea level) is located in the Turmot plain (Figure 1). According to the modern geographic regionalization, the study site belongs to the temperate semi-arid zone and the climate is mainly controlled by the Asian monsoon system. Turmot plain has a monsoonal climate with four clearly distinct seasons. Temperature and precipitation are positively correlated in the Inner Mongolian Plateau and both exhibit distinct seasonal variability characteristic of a monsoon climate. The rainfall is uneven throughout the year and concentrated in summer. Mean annual temperature is ~6.3ºC, and the annual mean precipitation is ~400 mm (Yun 1987). Local modern grassland vegetation is mainly *Stipa bungeana* and *S. breviflora.* The reeds (*Phragmites australis (Cav.) Trin. ex Steud*) were growing in the peat bog. The palynological composition of this bog is mainly *Artemisia, Chenopodiaceae* and *Ephedra* (Wang et al. 1997). The assemblage changed over time. Since 9.1 ka, the vegetation changed from the typical steppe-forest to steppe-mixed forest of coniferous and broad leave-forest-typical steppe (Wang et al. 1997). The Duoerji Peat bog is totally about 0.1 km^2 with hardly any water remaining in spring. We trenched in the middle of the bog, where there was no human tillage disturbance.

Sampling and AMS ^{14}C Dating

Our trenching in the Duoerji peat bog recovered a 237-cm sediment sequence composed of peat, clay and sand (Figure 2). The uppermost section, above 126 cm, is a dark brown peat that contained abundant undecomposed reed remains. Sediments below this level are black silty clay. Black sands occur at a depth of 159 cm and are followed by a yellow sand layer at 196 cm.

The chronology of the core was constructed from seven AMS ^{14}C measurements on organic matter. Bulk samples for radiocarbon (^{14}C) dating from selected levels were pretreated with 10% HCl and NaOH solutions, and then rinsed repeatedly with distilled water until neutral. They were then sieved through a 60 mesh (0.25 mm) sieve to remove fine sedge roots. Residual cellulose and leaf fragments were picked out and dried in an electric oven for ^{14}C dating. Details of this method are given in Zhou et al. (2002). Dating was conducted in the AMS Laboratory at the University of Arizona. Radiocarbon dates were calibrated using the CALIB 6.0 program (available at www.radiocarbon.org). The calibrated ages are quoted with two standard

https://doi.org/10.1017/RDC.2018.75 Published online by Cambridge University Press

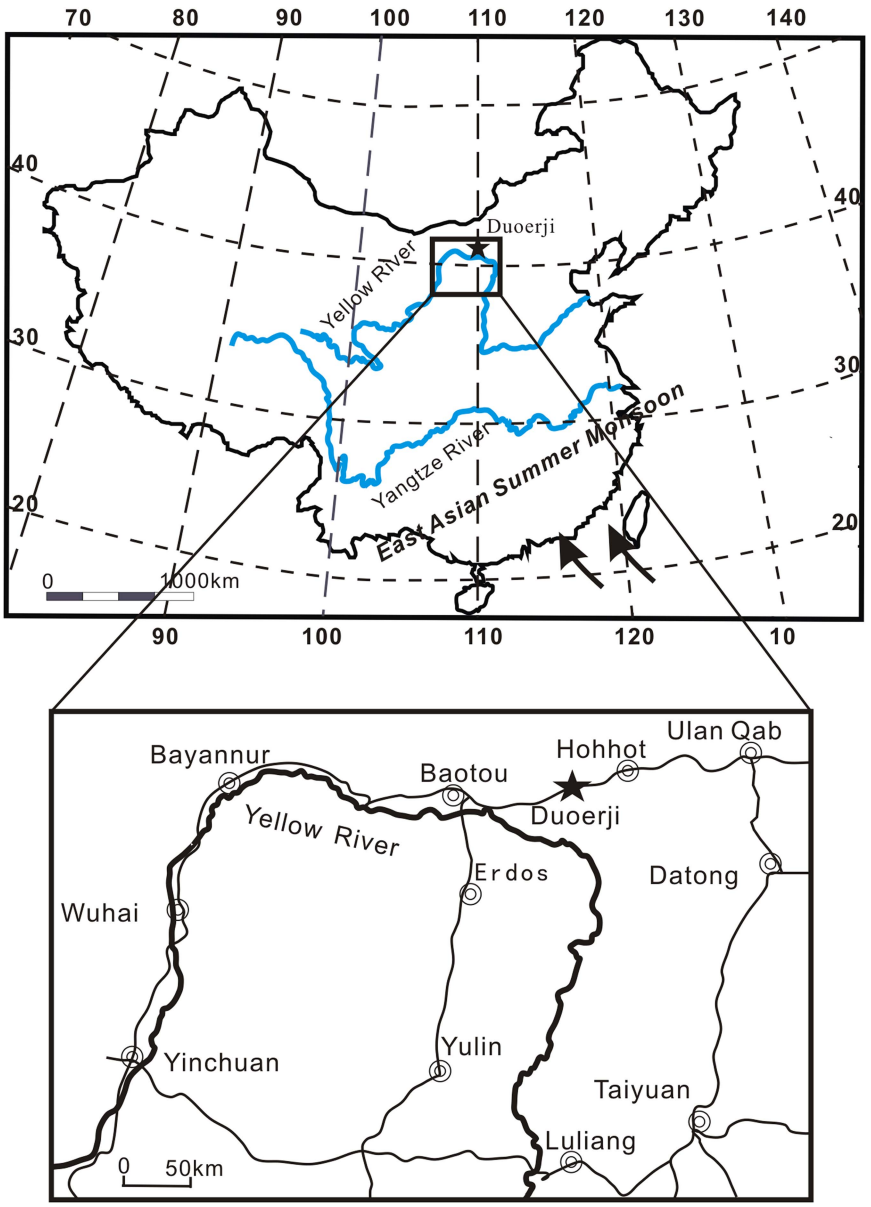

Figure 1 Location of the Duoerji peat bog.

deviation uncertainties (Table 1). We formulated an age-depth model based on median-probability ages of the calibrated dates using a cubic-spline regression method (Heegaard et al. 2005; Figure 2).

Sample Preparation

The solvent-extractable organic matter from 42 samples were prepared with an ultrasonic extractor using dichloromethane and methanol (volume ratio is 9:1) from 0.3 g freeze-dried

https://doi.org/10.1017/RDC.2018.75 Published online by Cambridge University Press

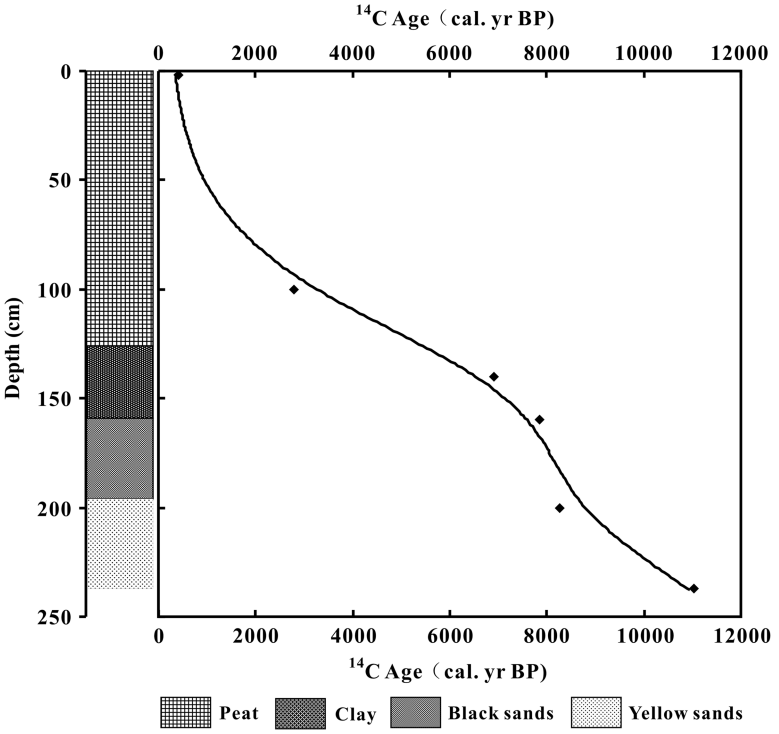

Figure 2 Calibrated AMS ^{14}C dates against depth of the Duoerji profile.

Table 1 Radiocarbon dates of the Duoerji sediment profile, Inner Mongolia.

Lab access ID	Depth (cm)	Materials dated	δ^{13}C (‰vs. PDB)	^{14}C age (yr BP)	Error	Calibrated age (yr BP)
AA95309	1	Peat	–27.7	507	±34	530
AA95310	2	Peat	–27.5	371	±33	434
AA95311	100	Peat	–26.9	2666	±36	2776
AA95312	140	Clay	–26.2	6208	±42	7100
AA95313	160	Black sands	–26.2	6853	±45	7684
AA95314	200	Yellow sands	–27.4	7497	±45	8323
AA95315	237	Yellow sands	–24.3	9720	±60	11148

peat or 5 g sand (3 × 30 min). The esterification of total extracts was processed by heating for 12 hr (60°C) with methanol hydrochloride. The samples were then dried under nitrogen, and extracted with hexane after adding a 5% sodium chloride solution. The total extract was separated using a solid phase extraction method on a silicagel column (200~400 mesh). Fatty acid methyl esters were eluted with dichloromethane (4 mL). The alkanes followed by elution with hexane (4 mL). The saturated fatty acid fraction was separated on another silicagel column (230 mesh) with 10% silver nitrate by eluting with 15 mL hexane and dichloromethane (volume ratio is 4:1).

https://doi.org/10.1017/RDC.2018.75 Published online by Cambridge University Press

Analysis of *n*-Fatty Acids

Lipid extraction, separation, and hydrogen isotope measurement were conducted in the State Key Laboratory of Loess and Quaternary Geology, Institute of Earth Environment, Chinese Academy of Sciences.

The components were identified and quantified using gas chromatography (Agilent GC 6890) with flame ionization detection (GC-FID) and an HP-1MS column (60 m × 0.32 mm × 0.25 μm). For quantification, peak areas for *n*-fatty acids were compared with those from an external *n*-fatty acids standard mixture. Hydrogen isotope ratios of individual compounds were determined using a Thermo Trace Ultra gas chromatograph with a Thermo Delta V Advantage isotope ratio mass spectrometer (GC-TC-IRMS). The individual compounds went to an isotope mass spectrometer, via quantitative conversion to H_2 in a high temperature oven operated at 1450°C. Compound-specific δD values were obtained using IRMS. The IRMS peak sizes were assessed by C_{24} acids. The peak sizes which ion beam of C_{24} acids >4000 mv were used for the analysis. The samples were measured in duplicates, and the average numbers were reported.

Methylated fatty acids were further derivatized as trimethylsilyl ethers using BSTFA (Sessions et al. 1999). Correction for the derivatization was calculated by using the following Equation (1) before reporting.

$$\delta D_{real} = [(2n+2) \times \delta D_{measured} + 123.7 \times 3] / (2n-1) \quad (1)$$

In Equation (1), n refers to carbon number of the studied compound, and δD_{real} is the true value of fatty acids, whereas $\delta D_{measured}$ is the measured value of fatty acids (Yang et al. 2003).

The δD values were normalized to the Vienna standard mean ocean water (VSMOW, D/H = $155.76 \pm 0.05 \times 10^{-6}$) scale using a standard mixture. δD is defined as

$$\delta D_{sample} = \left[(D/H)_{sample} - (D/H)_{std} \right] / (D/H)_{std} \times 1000 \quad (2)$$

C_{21}, C_{25}, C_{27},C_{29}, C_{31}, and C_{33} *n*-alkanes, purity ≥ 99.5% (Fluka Inc., Buchs, Switzerland), were used as experimental standards. Reproducibility and accuracy were evaluated by measuring *n*-alkane standards between every five measured samples, and the standard deviation of δD values of *n*-alkane standards was <3‰. To ensure stable ion source conditions during measurement the H_3 factor (Hilkert et al. 1999) was determined at least once a day, which was 4.12 ± 0.03.

RESULTS AND DISCUSSION

Distributions of *n*-Acids Extracted from Peat Samples from Duoerji Peat Profile

Carboxylic acids in sediment sequences originate from multiple sources. The nC_{16} and nC_{18} acids are ubiquitous components of biota, whereas the even chain C_{24}–C_{30} *n*-alkanoic acids originate principally from the waxy coatings of land plants (Cranwell 1974; Wiesenberg and Schwark 2006). Because carboxylic acids are more sensitive to degradation and modification than other types of lipid biomarkers (e.g., Meyers and Ishiwatari 1993), they can be useful indicators of the amount of organic matter recycling in subaqueous depositional sequences. As such, the acids serve as an important function in paleoenvironmental reconstructions by providing a relative measure of the reliability of source information from other biomarker compounds.

https://doi.org/10.1017/RDC.2018.75 Published online by Cambridge University Press

The chain length distributions for 42 samples from different lithologic units in Duoerji peat profile were analyzed on GC-FID. The compositions of *n*-acids range in chain length from nC_{16} to nC_{30} with distinct even-over-odd predominance (Figure 3). Most distributions are dominated

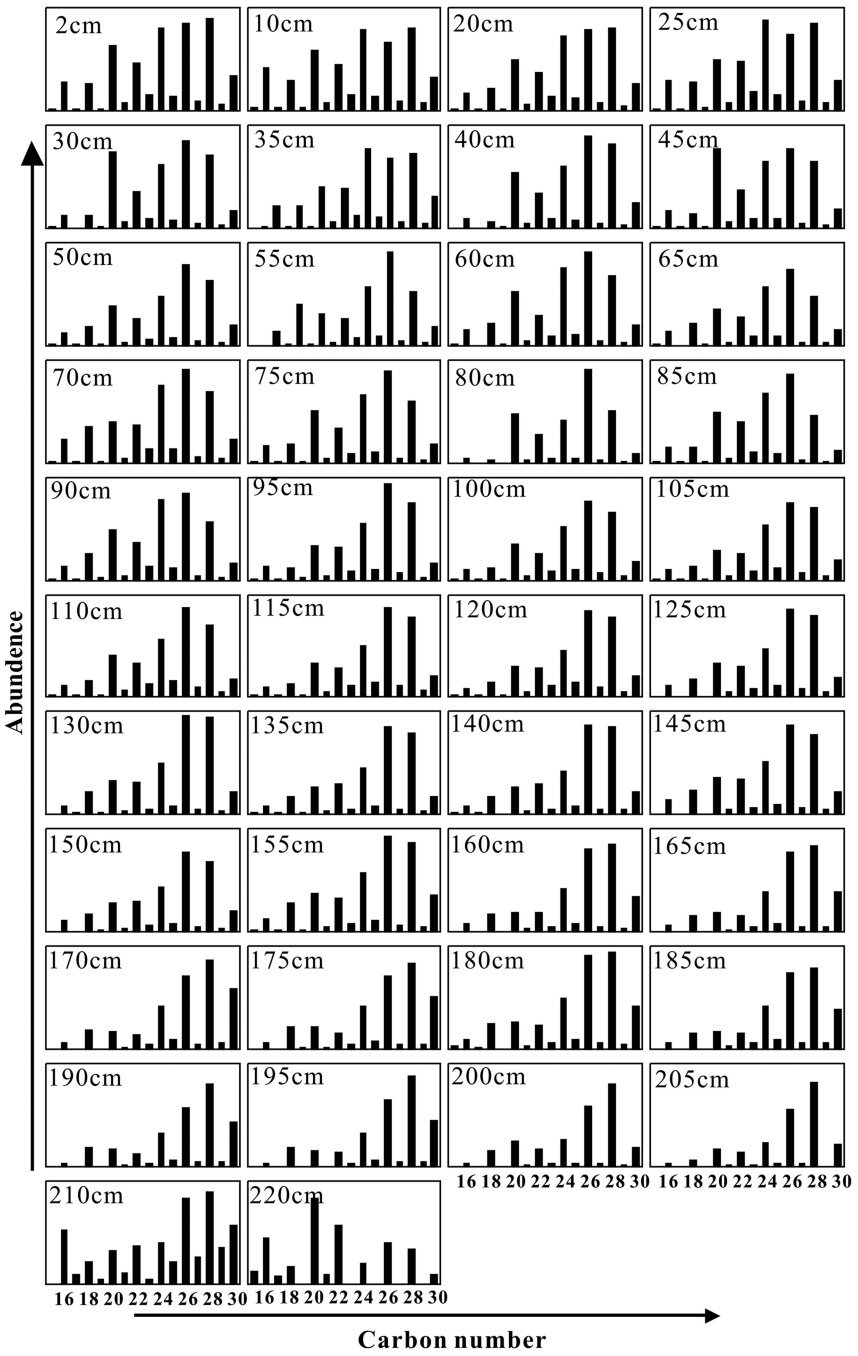

Figure 3 Distributions of *n*-acids extracted from peat samples from the Duoerji peat profile.

https://doi.org/10.1017/RDC.2018.75 Published online by Cambridge University Press

by the nC_{24}, nC_{26}, and nC_{28} components that are diagnostic of higher plants such as land plans and aquatic macrophytes. However, the proportions of *n*-acids in the distribution from the upper and bottom units were dominated by the ubiquitous nC_{20} and nC_{16} acids which suggested that it was largely derived from peat sphagnum. Their dominance throughout the sequence may indicate either preferential preservation relative to short chain algal fatty acids or dominance of land plant organic matter throughout most of the depositional history of the Duoerji bog sequence.

Variation in D/H Ratios of Plant-Derived *n*-Acids in Duoerji Profile and Biological Inputs

The δD records of *n*-C_{20}, *n*-C_{22}, *n*-C_{24}, *n*-C_{26}, and *n*-C_{28} acids show similar variation in the Duoerji sediment profile (Table 2, Figure 4). As the temporal resolution of our records are relatively low (28 sample over the past 10 ka), we focus on the general trend in this paper. We will analyze more samples in order to discuss the details. Over the past 10 ka, the δD

Table 2 Hydrogen isotopic composition of individual n-fatty acids from Duoerji sediment profile, Inner Mongolia.

		δD of *n*-fatty acids /‰, V-SMOW				
Sample ID	Depth (cm)	δD C_{20}	δD C_{22}	δD C_{24}	δD C_{26}	δD C_{28}
DEJ-2	2	−213	−214	−220	−227	−221
DEJ-10	10			−217	−225	−225
DEJ-20	20	−216	−219	−225	−231	−227
DEJ-30	30	−218	−216	−228	−241	−233
DEJ-40	40	−213		−229	−240	−235
DEJ-50	50	−221	−218	−225	−238	−231
DEJ-60	60	−219		−230	−236	−230
DEJ-70	70			−228	−234	−228
DEJ-80	80	−215	−213	−230	−242	−231
DEJ-90	90			−230	−236	−231
DEJ-100	100			−227	−235	−229
DEJ-105	105	−223		−231	−239	−238
DEJ-110	110			−232	−241	−233
DEJ-115	115	−226	−227	−238	−249	−247
DEJ-120	120			−235	−243	−241
DEJ-125	125	−226		−237	−248	−250
DEJ-130	130			−247	−250	−249
DEJ-135	135			−248	−253	−254
DEJ-140	140	−232	−225	−244	−248	−242
DEJ-145	145	−235	−228	−248	−253	−252
DEJ-150	150		−229	−245	−250	−246
DEJ-155	155	−240	−235	−252	−256	−256
DEJ-160	160	−241	−230	−251	−252	−250
DEJ-170	170			−250	−250	−252
DEJ-180	180			−244	−249	−249
DEJ-190	190			−250	−253	−255
DEJ-200	200			−251	−258	−262
DEJ-220	220	−228	−219		−210	−206
DEJ-plant	0	−211			−192	−202

https://doi.org/10.1017/RDC.2018.75 Published online by Cambridge University Press

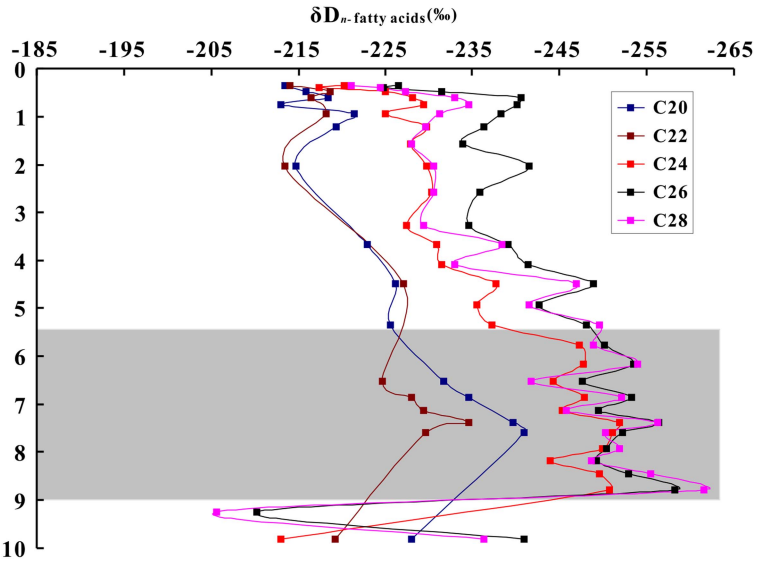

Figure 4 δD records of n-C20, n-C22, n-C24, n-C26, and n-C28 acids in the Duoerji sediments profile.

value of the n-C_{20} acid varied from –241‰ to –213‰ while the δD value of n-C_{22} acid varied from –234‰ to 213‰. The δD values of n-C_{24}, n-C_{26}, n-C_{28} fatty acids varied from –251‰ to –213‰, –258‰ to –210‰ and –262‰ to –206‰ (Figure 4). The amplitude of the δD values for n-C_{20} and n-C_{22} fatty acids were larger than n-C_{24}, n-C_{26} and n-C_{28} acids. The reason is still not clearly for us. During the Early Holocene (10–9 ka), the δD records of all acids were relatively enriched, and became depleted abruptly (> 50‰) at ~9 ka. δD of n-C_{26} and n-C_{28} acids reach their most remarkable depleted value at around 8.8 ka, while δD of n-C_{20}, n-C_{22}, and n-C_{24} acids reach their lowest value at around 7.5 ka. The δD values enriched gradually from 9 to 4.2 ka, then the δD values fluctuated slightly after 4.2 ka. Overall, the δD values are more depleted during the period 9–4.2 ka than between 4.2–0 ka. There are some gaps in the δD records of the n-C_{20} and n-C_{22} fatty acids as their abundance were too low to be detected in some samples.

Overall, δD values of the long-chain n-acids are smaller than short-chain n-acids. As long-chain fatty acids are mostly from higher plants (Cranwell 1974; Wiesenberg and Schwark 2006) such as emergent aquatic plant *Phragmites australis (Cav.) Trin. ex Steud.* and short-chain fatty acids are mostly from peat sphagnum, it can be deduced that the acids from peat sphagnum are richer in D than acids from reed. This difference has been shown to be common in the past. The hydrogen isotope compositions of herbaceous plants are smaller than symbiotic woody plants or bushes, as indicated by δD values of leaf wax n-alkanes in 34 modern plants from the Chinese Loess Plateau (Liu et al. 2006, 2008). The δD ratios of leaf wax compounds of over 70 plants around Blood Pond in Massachusetts, northeastern United States, were found to have leaf wax compound δD values that were 40‰ ~ 50‰ higher than herbaceous plants living under the same precipitation and photosynthesis conditions (Hou et al. 2007). Therefore, it is feasible to reconstruct the paleovegetation types by means of hydrogen isotopic compositions of leaf wax lipids in plants. In addition, new research suggests that differences between mid- and long-chain compound specific $\delta D_{n\text{-alkane}}$ values in lacustrine sediments can serve as a paleoclimatic indicator (Rao et al. 2014).

https://doi.org/10.1017/RDC.2018.75 Published online by Cambridge University Press

There are obvious sedimentological changes in the core, going from sands with less organic matter in the lower part through clays to bog peat rich in organic matter at the top. These changes in environmental and deposition settings could affect the plants that are producing the waxes and alter the isotopes. The distributions of *n*-acids and pollen records of Duoerji peat showed vegetation variation. The change to a bog at the end of the Holocene humid period possibly drove the enrichment of the δDwax to some extent.

Implications for Past Changes in the Precipitation in Inner Mongolia (10–0 cal ka BP)

Hydrogen in plant-derived *n*-acids is derived from the water source utilized by the plants. The D/H ratio of the *n*-acids is controlled by the isotopic composition of the source water and by kinetic isotopic fractionation that occurs during biosynthesis of the *n*-acids (Sachse et al. 2004; Seki et al. 2009). Meteoric water is the primary source of hydrogen for most plants, and its D/H ratio is determined by multiple environmental factors, including (1) the origin of the water and (2) the temperature, evaporation, and precipitation history of the air mass that delivered moisture the site (Craig 1961; Gat 1996). Because of their large mass difference, D and H are strongly fractionated in plants by environmental and biosynthetic process that is unlikely affected by the temperature. Evapotranspiration by land plants proceeds faster for H_2O than for DHO, with a consequence that deuterium becomes relatively enriched in leaf waters. This enrichment is variably influenced by humidity, making the δD values of land plant *n*-alkanes sensitive to climate change (Sachse et al. 2004; Hou et al. 2008). Unlike land plants, submerged plants that are immersed in water experience evapotranspiration less and their *n*-acid δD values are governed largely by the hydrogen isotopic composition of their host water (Sternberg 1988; Sessions et al. 1999; Huang et al. 2004; Hou et al. 2007). δD values of C_{28} *n*-alkanoic acids from a transect of 32 lake surface sediments across large gradients of precipitation show significant correlation with δD_P (precipitation D/H ratios) values ($R^2 = 0.76$) with an apparent isotopic enrichment of $\sim 99 \pm 8‰$, indicating that sedimentary δD wax values track overall δD_P variation along the entire transect (Hou et al. 2008). In addition, previous studies have confirmed that D/H ratios of lipid biomarkers from higher plants in the sediments in arid regions can be used to study precipitation changes (Mügler et al. 2008; Seki et al. 2009; Nichols et al. 2011).

The isotopic composition of precipitation in a given location is reversely correlated with the amount of rainfall, the classic "amount effect" (Dansgaard 1964). The amount effect in the Asian monsoon region is weaker than that in tropical inland (Araguás-Araguás et al. 2000; Bowen 2008), but it is still a significant factor influencing isotopic compositions of precipitation in China (Hoffmann and Heimann 1997). Though it was suggested that $\delta^{18}O$ of speleothems from eastern Asia does not inform on local precipitation amount or intensity because the isotopic excursion in precipitation is due to changes in the isotope composition of water vapor from different source regions, or mixed processes (Dayem et al. 2010; Battisti et al. 2015), the precipitation isotopes in China with intense summer monsoon precipitation are considered more dependent on the amount of precipitation than on temperature (Johnson and Ingram 2004; Liu et al. 2010; Yao et al. 2015).

In central Inner Mongolia, where climate conditions during the growing season are largely controlled by the East Asian monsoon, the isotope ratios are mainly controlled by the amount of precipitation with potential influence of temperature (Hoffmann and Heimann 1997). Though the influence of temperature on the δD fractionation for plant leaf waxes is small (Johnson and Ingram 2004; Liu et al. 2010), we can not fully exclude the influence of temperature on the variation of δD records. However, as the temperature and precipitation amount tend to vary similarly (An 2000), we focus on our discussion on the precipitation changes, which

https://doi.org/10.1017/RDC.2018.75 Published online by Cambridge University Press

in turn reflects the intensity of summer monsoon. High precipitation results in lower isotope ratios, which imply a relatively strong monsoon, while higher isotope ratios imply a relatively weak monsoon.

With these controlling factors in mind, we can draw the following conclusions from our δD records of the *n*-acids in Doerji peat (Figure 4).

Period 10–9 ka: The δD of *n*-C_{20}, *n*-C_{22}, *n*-C_{24}, *n*-C_{26} and *n*-C_{28} acids are all relatively high, as compared with the rest of the Holocene. This suggests that the precipitation in the Early Holocene was low and the climate was relatively dry.

Period 9–5.5 ka: All of the δD records of *n*-acids reached their lowest values in this period, recording a maximum precipitation value for the entire Holocene. This humid period was also reflected by the lithologic character of the sediments, composed of black sands and muds deposited when the water supply was abundant.

Period 5.5–0 ka: δD values of all of the *n*-acids increased steadily on a millennial timescale, since about 5.5 ka, with some smaller (~20‰) fluctuations on a centennial timescale. The overall trend indicates a gradual decrease in rainfall in the Late Holocene, as the climate becomes increasingly dry. Around 5.5 ka, the sediment in the profiles changed from a black silt layer to peat layer, indicating a shift in the sedimentary environment. That is a change from fluvial-lacustrine deposits to swamp deposits, as the regional water supply decreased. By analyzing the δD of the *n*-acids in modern reeds at the surface of the Doerji peat, we found that the δD of *n*-C_{20}, *n*-C_{26} and *n*-C_{28} were –211‰,–192‰, and –202‰, respectively, all higher values than the δD values of the corresponding *n*-acids in the down-core sediments. This suggests that the present climate in central Inner Mongolia is the driest we have observed.

The pollen assemblage from Duoerji peat suggested local vegetation experienced from typical steppe, through mixed coniferous broad leaved forest, and then back to typical steppe since 9.1 ka, (Wang et al. 1997), and reflected the paleoclimate changed through a sequence of cold–warm–cold, which is generally well compared with the dry–wet–dry sequence recorded by δD of *n*-acids.

In order to facilitate the following comparison and discussion, we calculated weighted average for *n*-C_{24}, C_{26}, C_{28} acids (δD_{wax}).

$$\delta D_{wax} = (W_{C24} \times \delta D_{C24} + W_{C26} \times \delta D_{C26} + W_{C28} \times \delta D_{C28}) / (W_{C24} + W_{C26} + W_{C28}) \quad (3)$$

δD_{wax} of the Doerji peat was compared with other monsoon records from the East Asian monsoon region in Figure 5, in order to identify consistent Holocene paleoclimatic patterns. The overall trend of the various paleoclimate proxies is consistent. The summer monsoon rapidly increased in the period 9–8 ka and a relatively strong summer monsoon persisted until about 5.5 ka. This period, between 9–5.5 ka is the Holocene Optimum for the East Asia monsoon region. During this period, the δD record of the *n*-C_{24} acid of the Duoerji peat reached its lowest value (Figure 5a), indicating a maximum summer monsoon rainfall value. This is also when magnetic susceptibility of Baxie loess section in Gansu Province reached its highest value (Zhou et al. 1992; Figure 5b), the $\delta^{18}O$ records of the stalagmites in Dongge cave in Guizhou reached their lowest value (Dykoski et al. 2005; Wang et al. 2005; Figure 5c) and the $(K_2O + CaO + MgO)/(SiO_2 + Al_2O_3 + TiO_2)$ of a lacustrine sediment profile in Daihai, Inner Mongolia, also reached a maximum value (Sun 2005; Figure 5d). Hence, paleomagnetic, isotopic, and geochemical proxies from a range of natural archives all reflect the intensity of the East Asian summer monsoon and the timing of the Holocene Optimum, a period of enhanced rainfall, soil

https://doi.org/10.1017/RDC.2018.75 Published online by Cambridge University Press

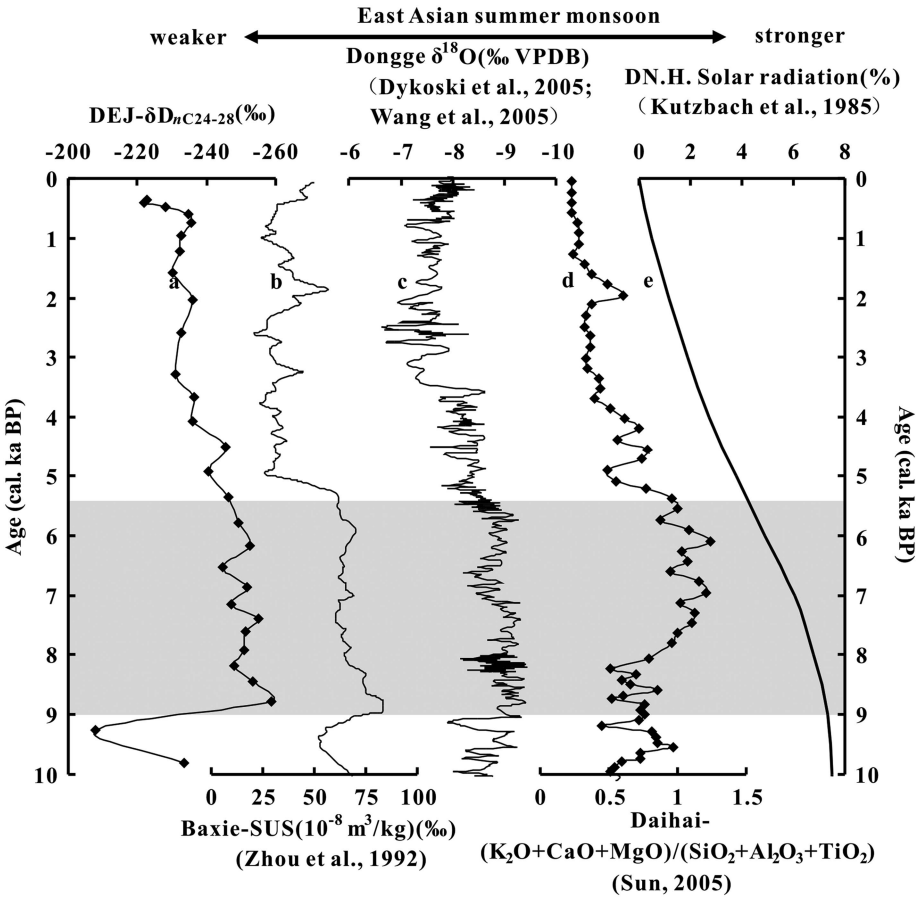

Figure 5 Comparison of various paleoclimate proxy records from East Asian summer monsoon region over the past 10 ka: (a) n-C24 acid δD records in Duoerji sediments; (b) Magnetic susceptibility of Baxie loess section (Zhou et al. 1992); (c) $(K_2O + CaO + MgO)/(SiO_2 + Al_2O_3 + TiO_2)$ of the lacustrine sediments in Daihai (Sun 2005); (d) maximum value; (e) summer insolation change at 30°N (Kutzbach et al. 1985).

development and chemical weathering. All the records show that the intensity of the East Asian summer monsoon gradually weakens after 5.5 ka, with an increasingly dry climate. It is also noteworthy that the δD of *n*-acids from Duoerji peat showed a relatively dry Early Holocene (10–9 ka, Figure 5a), which is not remarkable in Dongge cave record (Dykoski et al. 2005; Wang et al. 2005, Figure 5c). It could be true that they are real regional differences that reflect asynchronous Holocene optimum of the East Asian monsoon (An et al. 2000). It is also probably because Duoerji located nearby the arid Asian region where dominated today by the westerlies and experienced a dry Early Holocene (Chen et al. 2008).

Figure 5 shows the results of a small sample of studies that provide evidence for the Holocene Optimum in the East Asian monsoon and many other examples have been described in the literature. For example, the Xilinguole profile in Inner Mongolia also shows a humid period from 9–6 ka (Jin et al. 2004), and strata from Xiaoniuchang and Lake Haoluku at the south of the Hunshandake deserts record a humid period from 10–5.9 ka (Liu et al. 2002). As indicated by high and variable median grain size values and silt contents of Daihai lake sediments, the

https://doi.org/10.1017/RDC.2018.75 Published online by Cambridge University Press

Middle Holocene between ca. 7.9 and 3.1 ka was marked by intensified and highly variable monsoonal precipitation (Peng et al. 2005). Pollen-assemblage data from a sediment core from Hulun Lake in northeastern Inner Mongolia describe that grasses and birch forest expanded in 8000–6400 a BP, implying a remarkable increase in the monsoon precipitation (Wen et al. 2010).

Despite the correspondence between the above studies, the start and end of the Holocene Optimum appears to have a strong regional component, and sometimes divergent results are found in a single region. For example, diatom fossils from sediments in Lake Haolaihure, Inner Mongolia show that the warm and humid period 5.8–2.9 ka bracketed the Holocene Optimum (Guan et al. 2010), while a grain size study from Anguli Nuur Lake, on the southern margin of the Inner Mongolian Plateau shows that the most humid climate occurred from 10.4–7 ka (Yin et al. 2011). Perhaps these differences come from measurement uncertainties, chronological resolution, or proxy-specific issues. It could also be true that they are real regional differences that reflect an irregular northernmost margin of the East Asian monsoon. The existence of these contradictions will become clearer as additional paleoclimate records become available.

The millennial-scale trend of the East Asian monsoon records is in agreement with the solar radiation history for the Northern Hemisphere (Kutzbach et al. 1985. Figure 5e). The East Asian monsoon system responds quickly to summer solar radiation through the air-sea coupling, leading to climate change in the East Asian monsoon region. A cycle of insolation at much-lower frequency, resulting from progressive changes in the Earth's orbital parameters since the last glaciation, is likely to be reflected in a similar pattern of monsoon variation on a multi-millennial time scale. In the Early Holocene, the solar radiation for the Northern Hemisphere was enhanced, and then led to the ocean feedbacks to orbital forcing, caused the East Asian summer monsoon activity became stronger. In the Middle Holocene, the solar radiation turned to be reduced, resulting in East Asian summer monsoon weakening (An et al. 2000).

CONCLUSIONS

Changes of Holocene precipitation in middle Inner Mongolia are reflected in the D/H (δD) ratios of *n*-C_{20}, *n*-C_{22}, *n*-C_{24}, *n*-C_{26}, *n*-C_{28} acids. During 10–9 ka, higher δD values indicate relatively less precipitation, while the lowest δD, from 9–5.5 ka indicates a maximum in precipitation for the entire Holocene. After 5.5 ka, gradually increasing δD values indicate a continual decrease in regional precipitation with time.

The past changing trend of the hydrogen isotopic composition of the Duoerji peat is consistent with that of other major paleoclimate proxies in the East Asian monsoon region. Records from most study sites provide a consensus date for the Holocene optimum in the East Asian monsoon region from 9–5.5 ka. This period marks the strongest East Asian monsoon activity in the Holocene, and was followed by a gradual and continual drying climate, up to the present day.

ACKNOWLEDGMENTS

This work was jointly supported by the National Natural Science Foundation of China, the foundations from the Ministry of Science and Technology of China and Shaanxi Public Welfare Special Project of geological prospecting. We thank Dr. Shaohua Song and Dr. Zhao Liu for their help in the field work. We also thank Dr. Juzhi Hou for his useful discussions of this work. Additionally, we are grateful for the time and experience provided by reviewers and editors.

REFERENCES

An ZS. 2000. The history and variability of the East Asian paleomonsoon climate. *Quaternary Science Reviews* 19(1-5):171–87.

An ZS, Porter SC, Kutzbach JE, Wu XH, Wang SM, Liu XD, Li XQ, Zhou WJ. 2000. Asynchronous Holocene optimum of the East Asian monsoon. *Quaternary Science Review* 19:743–62.

Araguás-Araguás L, Froehlich K, Rozanski K. 2000. Deuterium and oxygen-18 isotope composition of precipitation and atmospheric moisture. *Hydrological Processes* 14:1341–55.

Battisti DS, Ding Q, Roe GH. 2015. Coherent pan-Asian climatic and isotopic response to orbital forcing of tropical insolation. *Journal of Geophysical Research Atmospheres* 119(21):11,997–12,020.

Bowen GJ. 2008. Spatial analysis of the intra-annual variation of precipitation isotope ratios and its climatological corollaries. *Journal of Geophysical Research* 113:D05113.

Brassell SC, Eglinton G, Marlowe IT, Pflaumann U, Sarnthein M. 1986. Molecular stratigraphy: a new tool for climatic assessment. *Nature* 320:129–33.

Bray EE, Evans ED. 1961. Distribution of n-paraffins as a clue to the recognition of source beds. *Geochimica et Cosmochimica Acta* 22:2–15.

Chen CTA, Lan HC, Lou JY, Chen YC. 2003. The dry Holocene megathermal in Inner Mongolia. *Palaeogeography, Palaeoclimatology, Palaeoecology* 19:181–200.

Chen FH, Yu ZC, Yang ML, Emi I, Wang S, David BM, Huang XZ, Yan Z, Tomonori SH, John BB, Ian B, Chen JH, An CB, Bernd W. 2008. Holocene moisture evolution in arid central Asia and its out-of-phase relationship with Asian monsoon history. *Quaternary Science Reviews* 27(3–4):351–64.

Clemens SC, Prell WL, Sun YB. 2010. Orbital-scale timing and mechanisms driving late Pleistocene Indo-Asian summer monsoons: reinterpreting cave speleothem $\delta^{18}O$. *Paleoceanography* 25:545–58.

Craig H. 1961. Isotopic variations in meteoric waters. *Science* 133:1702–3.

Cranwell PA. 1974. Monocarboxylic acids in lake sediments: Indicators, derived from terrestrial and aquatic biota, of paleoenvironmental trophic levels. *Chemical Geology* 14:1–14.

Cranwell PA. 1973. Chain-length distribution of *n*-alkanes from lake sediments in relation to post-glacial environmental change. *Freshwater Biology* 3:259–65.

Dansgaard W. 1964. Stable isotopes in precipitation. *Tellus* 16:436–68.

Dayem KE, Molnar P, Battisti DS, Roe GH. 2010. Lessons learned from oxygen isotopes in modern precipitation applied to interpretation of speleothem records of paleoclimate from eastern Asia. *Earth & Planetary Science Letters* 295(1–2):219–30.

Dykoski CA, Edward RL, Cheng H, Yuan DX, Cai YJ, Zhang ML, Lin YS, Qing JM, An ZS, Revenaugh J. 2005. A high-resolution, absolute-dated Holocene and deglacial Asian monsoon record from Donge Cave. *China Earth Planetary Science Letters* 233:71–86.

Eglinton G, Hamilton RJ. 1967. Leaf epicuticular waxes. *Science* 156:1322–34.

Ficken KJ, Street-Perrott FA, Perrott RA, Swain DL, Olago DO, Eglinton G. 1998. Glacial/interglacial variations in carbon cycling revealed by molecular and isotope stratigraphy of Lake Nkunga, Mt. Kenya, East Africa. *Organic Geochemistry* 29:1701–19.

Gat JR. 1996. Oxygen and hydrogen isotopes in the hydrologic cycle. *Annual Review of Earth and Planetary Sciences* 24:225–62.

Guan YY, Wamg Y, Yao PY, Chi ZQ, Zhao ZL. 2010. Environmental evolution since the Holocene in the Haolaihure antient lake, Keshitengqi, Inner Mongolia, China. *Geological Bulletin of China* 29:891–900.

Heegaard E, Birks HJB, Telford RJ. 2005. Relationships between calibrated ages and depth in stratigraphical sequences: an estimation procedure by mixed-effect regression. *The Holocene* 15:612–8.

Hoffmann G, Heimann M. 1997. Water isotope modeling in the Asian monsoon region. *Quaternary International* 37:115–28.

Hilkert AW, Douthitt CB, Schlüter HJ, Brand WA. 1999. Isotope ratio monitoring gas chromatography/mass spectrometry of D/H by high temperature conversion isotope ratio mass spectrometry. *Rapid Communications in Mass Spectrometry* 13 (13): 226–1230.

Hou JZ, D'Andrea WJ, Huang YS. 2008. Can sedimentary leaf waxes record D/H ratios of continental precipitation? Field, model, and experimental assessments. *Geochimica et Cosmochimica Acta* 72:3503–17.

Hou JZ, D'Andrea WJ, MacDonald D, Huang YS. 2007. Hydrogen isotopic variability in leaf waxes among terrestrial and aquatic plants around Blood Pond, Massachusetts (USA). *Organic Geochemistry* 38:977–84.

Huang YS, Shuman B, Wang Y, Webb T. 2004. Hydrogen isotope ratios of individual lipids in lake sediments as novel tracers of climatic and environmental change: a surface sediment test. *Journal of Paleolimnology* 31:363–75.

Ishiwatari R, Hirakawa Y, Uzaki M, Yamada K, Yada T. 1994. Organic geochemistry of the Japan Sea sediments 1: bulk organic matter and hydrocarbon analyses of Core KH-79-3, C-3 from the Oki Ridge for paleoenvironment assessments. *Journal of Oceanography* 50:179–95.

Jiang YJ, Wang W, Ma YZ, Li YY, Liu LN, He J. 2014. A preliminary study on Holocene climate change of Ordos plateau, as inferred by sedimentary record from Bojianghaizi lake of Inner Mongolia, China. *Quaternary Sciences* 34:654–65.

https://doi.org/10.1017/RDC.2018.75 Published online by Cambridge University Press

Jin HL, Su ZZ, Sun LY, Zhang H, Jin L. 2004. Holocene climatic change in Hunshandake desert. *Chinese Science Bulletin* 49:1730–5.

Johnson KR, Ingram BL. 2004. Spatial and temporal variability in the stable isotope systematics of modern precipitation in China: Implications for paleoclimate reconstructions. *Earth & Planetary Science Letters* 220:365–77.

Kutzbach JE, Street-Perrott FA. 1985. Milankovich forcing of fluctuations in the level of tropical lakes from 18 to 0 kyr BP. *Nature* 317:130–4.

Liu HY, Cui HT, Tian YH, Xu LH. 2002. Temporal-Spatial variances of Holocene precipitation at the marginal area of the East Asian Monsoon influences from pollen evidence. *Acta Botanica Sinica* 44:864–71.

Liu JR, Song XF, Yuan GF, Sun XM, Liu X, Wang SQ. 2010. Characteristics of $\delta^{18}O$ in precipitation over Eastern Monsoon China and the water vapor sources. *Chinese Science Bulletin* 55:200–11.

Liu WG, Yang H, Li LW. 2006. Hydrogen isotopic compositions of *n*-alkanes from terrestrial plants correlate with their ecological life forms. *Oecologia* 150(2):330–8.

Liu WG, Yang H. 2008. Multiple controls for the variability of hydrogen isotopic compositions in higher plant n-alkanes from modern ecosystems. *Global Change Biology* 14:2166–77.

Liu ZY, Wen XY, Brady EC, Otto-Bliesner B, Yu G, Lu HY, Cheng H, Wang YJ, Zheng WP, Ding YH, Edwards RL, Cheng J, Liu W, Yang Hao. 2014. Chinese cave records and the East Asia summer monsoon. *Quaternary Science Reviews* 83:115–28.

Logan GA, Smiley CJ, Eglinton G. 1995. Preservation of fossil leaf waxes in association with their source tissues, Clarkia, northern Idaho, USA. *Geochimica et Cosmochimica Acta* 59(4):751–63.

Meyers PA, Ishiwatari R. 1993. The Early Diagenesis of Organic Matter in Lacustrine Sediments. In: Engel MH, Macko SA, editors. Organic Geochemistry. New York: Plenum Press.

Mügler I, Sachse D, Werner M, Xu BQ, Wu GJ, Yao TD, Gleixner G. 2008. Effect of lake evaporation on δD values of Nam Co (Tibetan Plateau) and Holzmaar (Germany). *Organic Geochemistry* 39:711–29.

Nelson DM, Henderson AK, Huang YS, Hu FS. 2013. Influence of terrestrial vegetation on leaf wax δD of Holocene lake sediments. *Organic Geochemistry* 56:106–10.

Nichols J, Booth RK, Jackson ST, Pendall EG, Huang YS. 2011. Differential hydrogen isotopic ratios of sphagnum and vascular plant biomarkers in ombrotrophic peatlands as a quantitative proxy for precipitation-evaporation balance. *Geochimica et Cosmochimica Acta* 74:1407–16.

Peng YJ, Xiao JL, Nakamura T, Liu BL, Inouchi Y. 2005. Holocene East Asian monsoonal precipitation pattern revealed by grain-size distribution of core sediments of Daihai Lake in inner Mongolia of north-central China. *Earth & Planetary Science Letters* 233:467–79.

Rao ZG, Jia GD, Qiang MR, Zhao Yan. 2014. Assessment of the difference between mid- and long chain compound specific $\delta D_{n\text{-alkanes}}$ values in lacustrine sediments as a paleoclimatic indicator. *Original Research Article Organic Geochemistry* 76:104–17.

Ruddiman WF. 2008. *Earth's Climate, Past and Future*. 3rd edition. New York: Freeman and Company. p 1–17.

Sachse D, Radke J, Gleixner G. 2004. Hydrogen isotope ratios of recent lacustrine sedimentary *n*-alkanes record modern climate variability. *Geochimica et Cosmochimica Acta* 68:4877–89.

Seki O, Meyers PA, Kawamura K, Zheng YH, Zhou WJ. 2009. Hydrogen isotopic ratios of plant wax *n*-alkanes in a peat bog deposited in northeast China during the last 16 kyr. *Organic Geochemistry* 40:671–7.

Sessions AL, Burgoyne TW, Schimmelmann A, Hayes JM. 1999. Fractionation of hydrogen isotopes in lipid biosynthesis. *Organic Geochemistry* 30(9):1193–200.

Shi YF, Kong ZC, Wang SM, Tang LY, Wang FB, Yao TD, Zhao XT, Zhang PY, Shi SH. 1992. Climate fluctuations and important events of Holocene Megathermal in China. *Science in China Series B* 12:1300–7.

Sternberg L, da SL. 1988. D/H ratios of environmental water recorded by D/H ratios of plant lipids. *Nature* 333:59–61.

Sun QL, Wang SM, Zhou J, Shen J, Cheng P, Xie XP, Wu F. 2009. Lake surface fluctuations since the late glaciation at Lake Daihai, North central China: A direct indicator of hydrological process response to East Asian monsoon climate. *Quaternary International* 194:45–54.

Sun QL. 2005. Climate and environment evolution since the last Deglaciation recorded by the lacustrine sediments from Lake Daihai [PhD dissertation]. Graduate School of the Chinese Academy of Science (Institute of Earth Environment). In Chinese.

Wang FY, Sun XJ. 1997. A preliminary study on paleoenvironmental evolution during the Holocene from Chasuqi peat profile in Inner Mongolia. *Chinese Science Bullelin* 42:514–8. In Chinese.

Wang HY, Liu HY, Zhao FJ, Yin Y, Zhu JL, Ian S. 2012. Early- and mid-Holocene palaeoenvironments as revealed by mineral magnetic, geochemical and palynological data of sediments from Bai Nuur and Ulan Nuur, southeastern inner Mongolia Plateau, China. *Quaternary International* 250:100–18.

Wang YJ, Cheng H, Edwards RL, He YQ, Kong XG, An ZS, Wu JY, Kelly MJ, Dykoski CA, Li XD. 2005. The Holocene Asian Monsoon: links to solar changes and North Atlantic climate. *Science* 308:854–57.

https://doi.org/10.1017/RDC.2018.75 Published online by Cambridge University Press

Wen RL, Xiao JL, Chang ZG, Zhai DY, X QH, Li YC. 2010. Holocene climate changes in the mid-high-latitude-monsoon margin reflected by the pollen record from Hulun Lake, northeastern inner Mongolia. *Quaternary Research* 73:293–303.

Wiesenberg GLB, Schwark L. 2006. Carboxylic acid distribution patterns of temperate C3, and C4 crops. *Organic Geochemistry* 37(12):1973–82.

Xiao JL, Xu QH, Nakamura T, Yang XL, Liang WD, Inouchi Y. 2004. Holocene vegetation variation in the Daihai Lake region of north-central China: a direct indication of the Asian monsoon climatic history. *Quaternary Science Reviews* 2:1669–79.

Xu W, Cui LL, Xiao JL, Ding ZL. 2013. Stable carbon isotope of black carbon in lake sediments as an indicator of terrestrial environmental changes: An evaluation on paleorecord from Daihai Lake, Inner Mongolia, China. *Chemical Geology* 347:123–34.

Yang H, Huang YS. 2003. Preservation of lipid hydrogen isotope ratios in Miocene lacustrine sediments and plant fossils at Clarkia, northern Idaho, USA. *Organic Geochemistry* 34:413–23.

Yao Y, Yang H, Liu WG, Li XZ, Chen YW. 2015. Hydrological changes of the past 1400 years recorded in D of sedimentary *n*-alkanes from Poyang Lake, southeastern China. *Holocene* 518(3):94–9.

Yin Y, Liu HY, He SY, Zhao FJ, Zhu JL, Wang HY, Liu G, Wu XC. 2011. Patterns of local and regional grain size distribution and their application to Holocene climate reconstruction in semi-arid Inner Mongolia, China. *Palaeogeography, Palaeoclimatology, Palaeoecology* 307:168–76.

Yun H. 1987. *Country Annals of Turmot*. Inner Mongolia Peoples Publishing House. In Chinese.

Zhai DY, Xiao JL, Zhou L, Wen RL, Chang ZG, Wang X, Jin XD, Pang QQ, Shigeru I. 2011. Holocene East Asian monsoon variation inferred from species assemblage and shell chemistry of the ostracodes from Hulun Lake, Inner Mongolia. *Quaternary Research* 7:512–22.

Zhou WJ, An ZS, Lin BH, Xiao JL, Zhang JZ, Xie J, Zhou MF. 1992. Chronology of the Baxie loess profile and the history of monsoon climates in China between 17,000 and 6000 years BP. *Radiocarbon* 34:818–25.

Zhou WJ, Lu XF, Wu ZK, Deng L, Jull AJT, Donahue D, Beck JW. 2002. Peat record reflecting Holocene climatic change in the Zoige Plateau and AMS radiocarbon dating. *Chinese Science Bulletin* 47:66–70.

Zhou WJ, Yu XF, Jull AJT, Burr G, Xiao JY, Lu XF. 2004. High-resolution evidence from southern china of an Early Holocene optimum and a mid-Holocene dry event during the past 18,000 years. *Quaternary Research* 62:39–48.

Zhou WJ, Zheng YH, Meyers PA, Jull AJT, Xie SC. 2010. Postglacial climate-change record in biomarker lipid compositions of the Hani peat sequence, Northeastern China. *Earth & Planetary Science Letters* 294:37–46.

https://doi.org/10.1017/RDC.2018.75 Published online by Cambridge University Press